SECTION 51

DATA PROCESSING II: ADVANCEMENTS IN LARGE-SCALE DATA PROCESSING SYSTEMS FOR REMOTE SENSING*

by

David Landgrebe and Staff
Laboratory for Applications of Remote Sensing (LARS)
Purdue University
Lafayette, Indiana

INTRODUCTION

In the preceding paper, Dr. Swain described some of the research activities in Data Analysis techniques carried out at LARS/Purdue this past year. This paper continues by summarizing some results obtained from additional data processing research tasks now under study there. Time and space do not permit details. Full descriptions of these projects are reported in LARS reports and in papers in the open literature.

These studies fall into three categories: (1) an examination of the suitability of several sensor types with regard to producing data required for multispectral machine analysis; (2) various types of data preprocessing necessary to prepare such data for analysis in this fashion; and (3) an experiment in how to make this type of technology available efficiently and inexpensively.

COMPARISON OF SENSOR TYPES

There are a large number of different types of sensors capable of producing data as input to machine analysis processors. These sensor types tend to fall into three broad categories: scanners, photography and television. The line scanner tends to be preferred for this type of analysis procedure because it covers greater portions of the spectrum and has greater dynamic range and radiometric precision. However, scanners tend to be expensive, complex to operate and relatively unavailable at this time. Photography, on the other hand, is relatively less expensive and is widely available; it is a very well-developed technology.

---

*In this paper, results from a number of studies are summarized; researchers are identified in the Acknowledgment section.

Television has still different characteristics in this regard, having some of the advantages and disadvantages of both. In order to compare these sensors as sources of data for this type of machine processing and analysis, a scene was selected in which data had been gathered by both a scanner and photographic cameras simultaneously. Classifications with identical classes and training areas were carried out on both types of data. From this scene four different data types were to be compared:

- scanner data;
- black and white multispectral photography;
- color infrared photography; and
- vidicon-scanned color infrared photography.

The scanner data was used directly in this test. The black and white multispectral photography was first scanned, digitized and then the images from the several parts of the spectrum were registered with respect to one another. In the case of the color IR photography, color separations were first obtained and these were then scanned, digitized and registered.

Unfortunately, television data was not collected simultaneously with the other types of data since an airborne television sensor system was not available to us. However, in order to obtain some idea of how television might have performed, the color photography was subjected to a vidicon scanning system* after which it was digitized and registered.

The results of this study are shown in Figure 1 in bar graph form. The results for individual classes are shown on the left with the overall average results shown on the right. In carrying out this study, it was decided to assess the performance based upon the accuracy achieved by the samples used to train the classifier. This is compared to using so-called test samples or samples other than those used to train the classifier. It was felt in so doing that this would minimize the effect of scene variability, one of the other major experimental variables.

In the case of the scanner data, the best four of 15 available spectral bands were selected using the divergence processor. These bands turned out to be 0.44-0.46, 0.58-0.62, 1.0-1.4 and 1.5-1.8 micrometers. The data was collected with the Michigan scanner system. Three bands of black and white photography were available in a 70mm format. The film types and Wratten filters used were: Green, 2402, 58; Red, 2402, 25A; and IR, 2424, 89B. The color photography portion of the experiment was carried out using type 2443 color infrared film in a 9" by 9" format with a Wratten 15 filter.

---

*The vidicon scanning of the photography was accomplished by the IBM Houston Science Center at no cost to Purdue.

It is seen that the classification accuracy as a whole was very high. Thus, a two or three percent difference in overall accuracy is probably significant.

The results do tend to verify what might be expected from a detailed knowledge of the sensor type and processing algorithms, namely, that the scanner produced the highest performance. This was followed by the black and white multispectral photography; performance in this case was only slightly greater than color photography due no doubt to the possibility of achieving slightly greater radiometric precision with a single photographic emulsion as compared to a multiple-layer one. The television-scanned data gave the poorest performance, and while it must be kept in mind that this data contained the variability factors of both the photography and the television sensor, it nevertheless is to be expected that performance of a television sensor for this type of analysis would indeed be somewhat inferior to the others. No corrections were applied to the data with regard to sun angle effect, vignetting or other types of distorting factors.

DATA PREPROCESSING STUDIES

There are a large number of parameters of the sensor and data processing systems which are, at least initially, under the control of the system designer. Such factors as the spectral and spatial resolution, signal-to-noise ratio, the degree to which the signals are calibrated against available standards, and many others have a direct bearing upon the achievable classification accuracy. In order to determine the sensitivity and overall effect of the system with regard to these various parameters, a number of studies are underway at LARS/Purdue. An additional objective of these studies is the determining of suitable techniques by which data preprocessing may be carried out to modify and optimize the data with respect to these parameters. This is especially desirable since no one system design will be universally optimal for all data analysis purposes. Figure 2 shows the overall organization of these studies. They are divided into four broad areas, each of which has several sub-parts. For example, consider the programs in signal-to-noise ratio improvement indicated on the left. By using adjacent scan lines of data it is possible to improve the signal-to-noise ratio but, to some extent, at the expense of spatial resolution. This technique is used to remove or minimize the effect of such random noise as is generated in a scanner detector among other places.

There are many types of systematic noise introduced by sensors. Effects such as vignetting in photography or television where the data is collected in frames or Moire patterns in line scanners are examples

of problems which can be minimized or removed through data processing, but generally at the expense of other parameters in the system. The objective here is to develop suitable techniques to apply theory to practice and to quantify the result of doing so. In the remainder of this section are presented results obtained during the past year by several studies indicated in Figure 2.

SCANNER DATA CALIBRATION STUDY

Consider first a study of methods for the radiometric calibration of scanner data. The results from this study are shown in Figure 3. The data used for this study is from the Michigan scanner system and the 1971 Corn Blight Watch Experiment. With this scanner system the scanner sensors are optically exposed to three different calibration sources for each revolution of the scanning mirror. These are a black level (C_0), a level of fixed illumination (C_1) and a sensor exposed to the solar insolation on the top of the aircraft (C_2). The C_0 or black level calibration is intended to be used to remove any DC drift which may occur during the course of a data gathering mission by establishing a reference level at the output for zero (optical) energy in. It is possible to use either C_1 or C_2 to correct for any changes in system gain and/or any changes in illumination occurring at the top of the aircraft. In actuality, the computer software system used has been arranged in such a way that any two of these three signals can be used to establish calibration of the data in a linear fashion.

When considering data calibration however, one must recognize that calibration levels can only be determined with a signal-to-noise ratio which is finite (that is, less than infinite) just as is the case for the data from the scene itself. Thus, one will be using calibration information of a given signal-to-noise ratio to correct scene data of a given signal-to-noise ratio and depending on the need of the system for calibration, the effect may either improve or degrade the overall performance of the system. The question posed in this study then is: In a given situation does calibration help, and if so, which type helps the most?

Three different data sets were used in this particular test. These data sets are from segments 206, 208 and 215 of the 1971 Corn Blight Watch Experiment.* In each case training samples from a given segment

*Segments 201 through 230 of the 1971 Corn Blight Watch Experiment were distributed in order from north to south along the western third of the State of Indiana. These three segments are therefore from the northern half of the state and are separated by a maximum of about 100 miles. Each segment is approximately 1 by 8 miles.

were selected for a corn vs. noncorn classification. The classification was carried out and then samples from fields other than those used for training were used to test the accuracy to assess the performance.

Shown in Figure 3 are the results of the test with the individual segment accuracies shown on the left and the overall average shown on the right. The overall average does indeed indicate that calibration helps, although note that in segment 215 the "no calibration" control classification provided a higher performance than any of the types of calibration. Again, overall there was indicated a slight preference for using the $C_0 - C_1$ calibration.

Based on the design of the sensor system, the signal-to-noise ratio of the C_1 calibration signal is, in general, poorer than that from the sun sensor C_2. That is to say, given a higher quality signal from the calibration lamp, this slight preference in this case of $C_0 - C_1$ calibration might become an even more pronounced preference. It is important to add however, that in the case of aircraft data, as one collects data from larger and larger areas, variations in solar illumination become more important, and it may become more desirable to use $C_0 - C_2$ calibration in order to achieve highest accuracy. This proved to be the case in the next experiment to be described.

EXTRAPOLATION OF TRAINING SAMPLES

Over how large a geographical area is a given training set valid? This is a very important question. Only a relatively small proportion of the total cost of processing the data at the present time is attributable to the actual analysis calculation itself. This is true whether the analysis is done by analog or digital mode. The expensive portion of the processing remains the training phase of the analysis. Thus, it is important to develop techniques which reduce the complexity and therefore the cost of the training phase and it is also desirable to develop techniques by which a single training of a classifier can be utilized over larger and larger geographical areas. It was an examination of this latter question which was treated in the study to be described now. Many of the details of the study are apparent from the results displayed in Figure 4. The ordinate displays test data accuracy. The abscissa indicates the segment of the 1971 Corn Blight Watch Experiment data from which training was derived. The legend of the graph indicates the segments classified. The following table indicates the distance separating each segment.

Number of Airmiles Separating the
Center of Four Segments of the
1971 Corn Blight Watch Experiment

Segment Number	208	215	230
206	28	90	235
208		68	193
215			126

As expected, it appears to be generally true that the farther one gets from the training sample area the poorer the accuracy. However, there are several factors to be kept in mind in this particular test in considering how rapidly the accuracy deteriorates with distance. First of all, the segments are distributed in a north-south direction. This is the direction of maximum change with regard to seasonal variation. One would expect the growing season to be approximately two weeks further advanced at the southern most segment on a given day than at the northern most. Second, while all data used is from the same mission period of the corn blight watch, it did not prove possible to gather all the data on the same day. Indeed, the data gathering was extended over a 13-day period and, in addition, the data from the north, or least advanced portion of the growing season, was gathered first, with that in the south or most advanced being gathered last. This tended to enhance seasonal variations with regard to crop maturity. All data was gathered between 10:30 and 11:45 a.m. Thus there were only relatively small changes in sun angle. It did prove desirable in this case to use $C_0 - C_2$ calibration. That is, that calibration involving removing DC drift with the black level calibration information and adjusting the overall system gain based upon the indicated solar illumination as determined at the top of the airplane.

These results together with earlier results shown, tend to be encouraging with regard to the extrapolation of training sets particularly in view of the improvement expected when satellite-gathered data becomes available. Perhaps one of the greatest advantages of the satellite, one which is not achievable with an aircraft system, is that data over very large areas can be gathered in a very short time, thus holding as nearly constant as possible many experimental variables of the system such as the sun angle, time of the growing season, etc.

SUN ANGLE EFFECT CORRECTION

Attention has often been drawn to the fact that the reflectance of earth surface materials is very dependent upon the angle of illumination relative to the angle of view. This fact has a pronounced effect upon all types of imagery. The effect on scanner imagery is illustrated in Figure 5. The left image in this figure shows uncorrected data which was gathered by scanner at 10:00 a.m. This data was gathered from an aircraft having a northern heading such that at this hour of the morning the sun was to the right and somewhat to the rear (due to the season and latitude of the flightline) of the aircraft. The fact that the image appears washed out on the left is not an artifact of image reproduction, but sun angle effect which is present in the data.

Briefly, since the line of view is nearly parallel to the illuminating rays of the sun on the left portion of the image, the amount of energy reflected from any given (rough surface) material tends to be greater.

This effect is even more apparent by viewing the average response from a large number of scan lines. Figure 6 shows such a presentation in graphical form. Plotted here is the average response for a large number of columns of data in the imagery plotted versus the column number. For this data set, gathered shortly after 9:00 a.m., the response is clearly greater on the left, or west, portion of the field of view than it is on the right, or east. Figure 7 and 8 show presentations of the same type for data gathered near local noon and late in the afternoon, respectively. Variations of this effect with time of day is readily apparent.

This effect has been known for some time and it is relatively easy to improve the appearance of the imagery by appropriate processing. The most successful technique found to date has been to use a characteristic curve such as Figure 6 to derive appropriate multiplicative correction factors for each column in the data. The results of having applied this technique to the data for the leftmost image of Figure 5 is shown in the center of Figure 5. It is obvious that the appearance of the image is greatly improved. However, a careful inspection of the image will reveal that a vertical line structure has been introduced into it due to the fact that the characteristic curve was not sufficiently smooth. If, prior to applying the correction, this characteristic curve is smoothed appropriately, the result achieved will be as shown in the right-hand image of Figure 5.

Perhaps more important than the appearance of the image, however, is the quality of the data itself. A more quantitative test of the relative effectiveness of this type of correction can be obtained by carrying out a classification of the data set into appropriate classes for the case

of both corrected and uncorrected data. Two examples of the result of doing this are shown in Figure 9. In this case, the results for a corn versus noncorn classification carried out on two different data sets is shown, and in each case the classification of the original versus sun-angle-corrected data is compared. Note that the correction of the data did result in a significant improvement in accuracy for the classification indicated by the two pair of bars on the left. However, the other classification shows a degradation of performance due to data correction. Note that the degradation occurred in the data set collected earlier in the morning, when the sun angle effect would be more severe.

The purpose of this is to illustrate the point that though satisfactory improvement in image appearance is possible, the results with regard to improving data quality are quite mixed. It must be kept in mind that the degree to which the illustrated sun angle effect takes place depends not only upon the angle relationship between the sun, the scene and the observer but also the contents of the scene itself. Individual areas within the scene will display this effect to a greater extent depending on their contents. By the procedure described, although a globally appropriate correction can be made, there is no information available by which to make the correction also locally correct. Since classification is made on a local basis it is local correction that is required. Best overall results can be obtained by defining pairs of classes - one set for the left side of the scene, the other for the right side - but at the expense of training and processing complexity. It is felt, therefore, that the problem is in an unsatisfactory state and a new approach is really needed, one no doubt less empirically based, but based on an appropriate model of the total situation.

DATA COMPRESSION TECHNIQUES

We turn now to the question of data compression. One of the most obvious characteristics of the remote sensing field is the large quantity of data. This data quantity tends to strain system resources especially with regard to data transmission and data storage and retrieval. If means for compressing the data can be found which do not significantly alter the data quality, it would be most valuable. This led us to begin a data compression study and in particular to examine a class of linear transformations for this purpose. Among other advantages, this approach would tend to minimize the amount of additional processing which would be involved.

There exists in the literature a particular signal representation scheme known as the Karhunen-Loeve Orthogonal expansion. Theoretical results available with regard to this expansion suggested a number of advantages and I shall briefly describe the technique. In this

application it amounts simply to a principal components transformation and this is illustrated in Figure 10. Suppose for example, we have some multispectral data in two spectral bands. Since multispectral data is typically correlated from channel to channel it may distribute itself as shown by the oval shaped distribution in this figure. A principal components transformation amounts to defining a new set of axes by taking a linear combination of the original axes. The computation involved is shown by the two equations in the lower part of the figure. The a coefficients in these equations determine the orientation of the new axes relative to the original ones.

A principal components transformation is that particular transformation by which the first new axis, y_1 in the figure, is chosen so as to be oriented along the direction of maximum range or spread of the data as shown in the figure. The second component is chosen perpendicular to the first but in the direction of the next most principal distribution of the data. In higher dimensional cases, succeeding axes continue to be chosen orthogonal to the prior ones but in the direction of maximum remaining range of distribution.

The usefulness of this transformation for the data compression problem comes about because multispectral data, typically being highly correlated between spectral bands, tends to fall in a relatively long, narrow distribution in n-dimensional space. Thus, it is possible to concentrate most of the dynamic variability of the data in a very few number of principal components. This is dramatically illustrated in Figure 11, which is a plot of one measure of the dynamic range of the data after transformation as a function of the principal component number. This data was from 12 spectral bands and it can be seen that after transformation only about 3 coordinates have any appreciable dynamic distribution of data. The concept for data compression purposes is to transform this 12-spectral band data into 12 new components and then discard the, in this case 9, which have essentially no range and therefore no information in them. In this case, a 12 to 3 or 4 to 1 compression ratio would be achieved while incurring only the small error indicated by the sum of the mean square values of the 9 discarded components as compared to the 3 retained ones.

A further compression can also be achieved by a process called "bit allocation." For example, suppose the original 12 band data had been represented to an 8 bit precision in each of the 12 bands; that is, in each band any one of 256 possible gray values is allowed for. This would be 8 bits times 12 bands or 96 bits per multispectral sample.

Again referring to Figure 11, certainly the dynamic range of the first principal component after transformation would be much larger than any of the original spectral bands had been. Therefore, in order to

achieve the same precision of data representation more bits would need to be assigned to this component. However, succeedingly less could be assigned to successive components. It may turn out, for example, that for the 3 most principal components, the dynamic range required in terms of the number of bits might be 9, 6 and 4 allowing for 512, 64 and 16 gray values respectively for the three most principal components. This total new bit allocation of 9 plus 6 plus 4 equals 19 bits and compares with the 8 plus 8 plus 8 equals 24 which might have been used had not bit allocation been considered. This represents not only an additional compression of data but also an improvement in the precision with which the data would be presented since the original 8 bits in the first principal component would not have been adequate to handle properly the larger dynamic range.

Figure 12 shows a block diagram of a test data compression system which has been assembled in order to test this general approach on earth resources multispectral data. The first two blocks indicate the two steps just described; namely, data transformation followed by bit allocation. If it is then desired to recover the original data, the next step would be an inverse transformation followed by a bit allocation, thus transforming the compressed data back to the original coordinate system and the original dynamic range.

Two additional features not previously described have been incorporated into this system. First of all, though the above description of the concept involves compression based only on spectral redundancy, it is possible to use this approach to take advantage of both spectral redundancy and spatial redundancy in the imagery data. It is apparent from the above description that basically the only requirement at the input is for the data to be in the form of a vector representation. The components of the vector may be spectral components as described above, but they may also have been derived by using groups of vectors in spatial proximity to one another. For example, if the data is composed of samples from a 12-band multispectral scanner, inputs to this data compression system could be assembled by taking pairs of adjacent points, thus creating 24-dimensional input vectors. Indeed, the system of Figure 12 is prepared to handle data from an arbitrary number of lines, an arbitrary number of columns and an arbitrary number of channels of adjacent sample points. In this way, in addition to spectral redundancy, spatial redundancy can also be used to achieve higher compression ratios.

Another feature of the system is that other transformations besides the Karhunen-Loeve (principal components) transformation have been implemented with the system. The principal components transformation is a type referred to as a data-dependent transformation in that the precise coefficients for the transformation are computed each time based upon calculations involving the total data set to be transformed. However, any transformation could be used and at least two other transformations

have been examined besides the one just described. These are the standard Fourier (harmonic analysis) transformation and one called the Hadamard transform. The Fourier transform was selected for tests because of its familiarity and the robustness the transformation has shown with regard to a large class of problems extending across the various fields of science. The Hadamard transform, on the other hand, was selected because of its extreme convenience since the Hadamard functions and, therefore, the coefficients involved, are always either ones or zeros, thus making a digital implementation of this transform extremely simple and efficient from the computational standpoint. Both of these two transforms are non-data dependent; that is, they require no prior computation of scene statistics before proceeding with the transformation. In addition to these two, an "average" Karhunen-Loeve transform could be used based on scene statistics from a so-called average scene. This would be another means of eliminating a need for a precalculation of scene statistics at the cost of some degradation from optimum performance.

In addition to data compression for data storage and retrieval purposes, a procedure such as the above could have several other advantages. For example, in Figure 12 the data transformation output could be used directly for feature selection and classification purposes. Assuming 12-dimensional original data, one problem immediately to be faced in preparing to analyze the data set is which spectral bands will be best in a given classification. A somewhat lengthy computational procedure is available for determining the optimum subset of spectral bands desirable; however, the data in principal components form can be used directly in that the first n-principal components tend always to produce classification accuracies which are at or above the accuracy performance obtainable by the same number of optimally chosen original spectral bands. Thus, in addition to accomplishing data compression, this scheme shows promise for eliminating the need for the optimum feature selection computation. This property of the transformation has been known for some time and has been used previously by other researchers elsewhere.

Further, since after data transformation the coordinate system, and therefore the components involved, have been oriented to have maximum dynamic range, if an image is constructed using the data from the first principal component at this point, the image will have greater dynamic range and therefore greatest scene contrast of any possible image presentation of the data. One is guaranteed of having greater image contrast than any one of the original spectral bands could have. This provides imagery useful in determining, for example, boundaries in the scene and manually determining differences between any two materials. Figure 13 shows images constructed from data using the first, second, third and twelfth principal components. These images were produced by attempting to spread whatever dynamic range is present in the data over the full range of the contrast available in the photographic film. Notice that the scene contrast of the first principal component image is markedly greater than that in the third

and slightly greater than that in the second. Notice also that the twelfth principal component has essentially no image detail at all.

How does one determine the effectiveness of a proposed data compression scheme? The questions which must be asked are: how much distortion does the compression scheme introduce into the data and how much does this distortion affect the potential classification accuracy and the image quality. Figure 14 gives the rate distortion characteristics for this compression scheme and therefore shows the relationship of the degree of compression obtained to the amount of distortion introduced. The distortion is assessed by determining the mean square difference between the original image and the compressed and reconstructed image. In this case, the original data was available at eight bits-per-sample precision. In this case, the lower and upper curves are bounds on possible performance. The lower curve represents a best performance theoretical limit based upon information theory considerations after appropriate assumptions. The upper curve on the other hand, is the result achieved by simply truncating the number of bits per sample in the data. In between them, then, lies the performance characteristics for the three transformations under consideration. The Karhunen-Loeve clearly provides the best performance. However, keep in mind that it is a data dependent transformation. The Fourier and Hadamard transforms show the penalty of achieving non-data dependency. These are the performance characteristics based upon using a rectangular region out of the image of size 8 samples by 8 samples by 2 spectral bands to construct the vector which undergoes the transformation. This appears to be a near optimal choice of combination between spectral and spatial redundancy.

Figure 15 shows the results of carrying out classification tests on the compressed data. A test classification was carried out using various numbers of features. In the case of the original data, the optimal spectral bands were first determined in each case. On the other hand, in the case of the principal components data, components were added in order as higher dimensional classifications were desired, thus indicating the lack of necessity for the calculation of optimal spectral bands in this case. Notice that the principal component classifications were always at least as high and usually higher in performance compared to the same number of components of original data. Notice also that the classification with three spectral bands was approximately as high as that achieved with any number of bands.

And finally, Figure 16 shows the result of carrying out a compression by a factor of eight and then reconstructing the image from the data. This is compared with the image made from the original data. For the small amount of distortion present, keep in mind that with such a procedure if it had originally been required to have 8 digital tapes to store the data, using this procedure only one would be necessary.

TEMPORAL INFORMATION AND THE IMAGE OVERLAY PROCESS

During each of the previous of these annual meetings, we have reported on progress towards achieving a suitable capability for the precision overlaying of one image from a given geographic area onto that of another from the same area. These images may be from different parts of the spectrum and/or from data gathered at a different time. This has proved to be very challenging, primarily since the precision required is better than plus or minus one resolution element; thus, in the overlay process one must cause all local distortions of one image to precisely conform to those of the other.

Though this processing step is likely to be a relatively expensive one in terms of achieving image overlays of this precision, there are a number of important advantages which will accrue as a result. For example, temporal information could be made available to the processor by having images from different time periods registered with respect to one another. Also, the need to correlate ground truth information with data from a new mission can be eliminated by overlaying the new image data onto an image for which the correlation has already been established. And, in the case of airborne scanner data which often contains unexceptably high geometric distortions, these distortions can be removed by simply overlaying them onto an image which is of high geometric quality. By overlaying the new data onto existing maps of areas, procedures could be established whereby the maps could be automatically updated after subsequent analysis of the data.

Before describing new procedures developed this past year for improving overlay quality possible, an example result in the use of temporal information will be shown. This result is given in Figure 17. Data from Missions 43M, 44M, 45M and 46M of the University of Michigan airborne scanner system and the 1971 Corn Blight Watch Experiment gathered over segment 208 were overlayed upon one another. This figure shows the result of carrying out classifications for corn versus non-corn for various subsets of features in this total data set.

First of all, beginning on the left, classifications for each individual mission period were carried out using the best four channels from each mission period as chosen by the divergence processor. It is seen that the performance was relatively high on Mission 43 but dropped considerably by the next mission and then began a slow rise. In addition to indicating that some times of the growing season are better for making these discriminations than others, part of the difference in performance in these four classifications is due to differences in quality of the data due to such factors as weather conditions, etc.

The fifth set of bar graphs indicates the result of using all of the preceding data for a classification; that is, a 16-band classification, each four of which came from a different mission period. Notice that the capability for classifying corn and the overall accuracy was indeed considerably higher in this case.

One additional question has been posed of this data set so far. It was hypothesized that not all 16 channels were necessary; that is, that the data is not really intrinsically 16-dimensional. The last classification was carried out using the best four of the 16 channels. The results show an overall performance down from the previous classification and also down from the results obtained for Mission 43M alone. This would tend to suggest that more than 4 of the 16 bands are indeed significant in this case. Much more needs to be determined about temporal information and its value.

With regard to the overlay procedure itself, a new element has been added to the technique in order that a larger number of different situations can be successfully handled. This work began originally with scanner data in mind. More recently, scanned photography and television imagery have also been successfully overlayed.

Figure 18 shows the steps now used in the overlay procedure. First, initial checkpoints or points of obvious image congruency are marked manually. Based on these checkpoints in the two images to be overlayed, a curve-fitting operation is carried out to find the best fit between the images from this initial information. More specifically, several coefficients in the curve-fitting operation are computed. Next, a fast fourier transform two-dimensional correlation is carried out between the two images over a uniform grid to obtain precision checkpoints. This correlation uses the initial overlay previously determined by the checkpoints in order to minimize the region which must be searched for a maximum of correlation. As a result of this correlation operation, a final overlay function is computed and the two images are then merged to achieve the final overlay of the images.

Figure 19 shows the actual overlay function which would be required for some photographic data from the Apollo 9 S065 experiment. Briefly, frame 3808 from the Lubbock, Texas area was scanned and digitized at a rate of approximately 2100 scan lines by 2100 samples per scan line. Shown here in the two curves is the variation in registration in terms of columns (samples). From the upper curve, it is seen that for channels 1 and 2, the green and red, respectively, when the left edge and right edge of the two images were in proper registration, the center of the frame was out of registration by as much as four samples. On the other hand, from the lower curve comparing channel 1 with channel 3, the green with the infrared respectively, the misregistration in this case was also

by as much as four samples but in the opposite direction. Thus, it would be necessary to change the local distortion of the red and the infrared channels so that it more properly corresponds with the green channel prior to the actual image overlay process. The entire process is, of course, carried out digitally.

ON THE AVAILABILITY OF TECHNOLOGY

One final experiment which is now underway will be described. The problem is as follows: research into techniques for the machine processing of earth resources data has now been underway for several years and significant new technology is now available. How can this technology become available to the user community? In considering this question, it was decided to analyze how this had been accomplished at Purdue between the data processing specialists and user scientists.

The elements for the availability of this technology are hardware, software and the knowledge or training on how to use the system. Hardware, at least in the form of general purpose computers, is readily available, but expensive. The transfer of software is more of a problem. The implementation of a large software system on a new computer is a relatively expensive process requiring special data processing expertise. It is also relatively expensive to maintain the software once it has been implemented.

Insofar as the third element, training, is concerned, it was possible at LARS to give individual attention to training each new staff member in the use of the system. However, for the transfer of technology to a large body of people, this technique would be too expensive and slow. This led to the proposal of a specific experiment in the transfer of technology. The concept is illustrated in Figure 20. It became apparent that the hardware a user scientist needs to have available is a card reader and punch, a typewriter and a line printer, in short, the I/O devices. Thus, it is possible to centralize not only the computational capability, but also the data storage capability required. Such a system would then have the following advantages: (1) full user access to both the data and the processing capability at the user's location; (2) centralization of the expensive portions of the hardware at considerable cost advantages; (3) centralization of software maintenance, again achieving a cost advantage plus a flexibility in updating; and (4) facilitation of training through commonality of data format, terminology and simplicity of communication. As a result of this commonality, standard training materials tailored to the specific system could be developed and the amount of teacher time per pupil could be greatly reduced by relying on training materials. The computer itself can be used for training purposes through computer-aided instruction.

The status of this experiment is as follows. It was authorized by NASA/Headquarters two years ago. On January 1, 1971, an IBM System/360 Model 67 time share system was placed on line in a minimal configuration in order to appropriately prepare the software system. The 1971 Corn Blight Watch Experiment necessitated a delay in the experiment since both the equipment and the personnel involved were required for the Watch. However, recently the final hardware was installed and is now ready. Some training materials are already ready while others are in preparation. The location for the first terminals are now being selected by NASA/HQ. It is expected that the experiment will be underway by the time ERTS is launched.

ACKNOWLEDGMENT

The research summarized herein was supported by NASA under Grant NGL 15-005-112. Grateful appreciation is expressed to NASA for this support. The various individual studies were carried out by Mr. Paul Anuta, Patrick Ready, a graduate student, Mr. Terry Phillips, David Strahorn, a student, Professor Paul Wintz, Dr. Stanton Yao and the author. Mr. Phillips has overall responsibility for coordinating the research projects reported here.

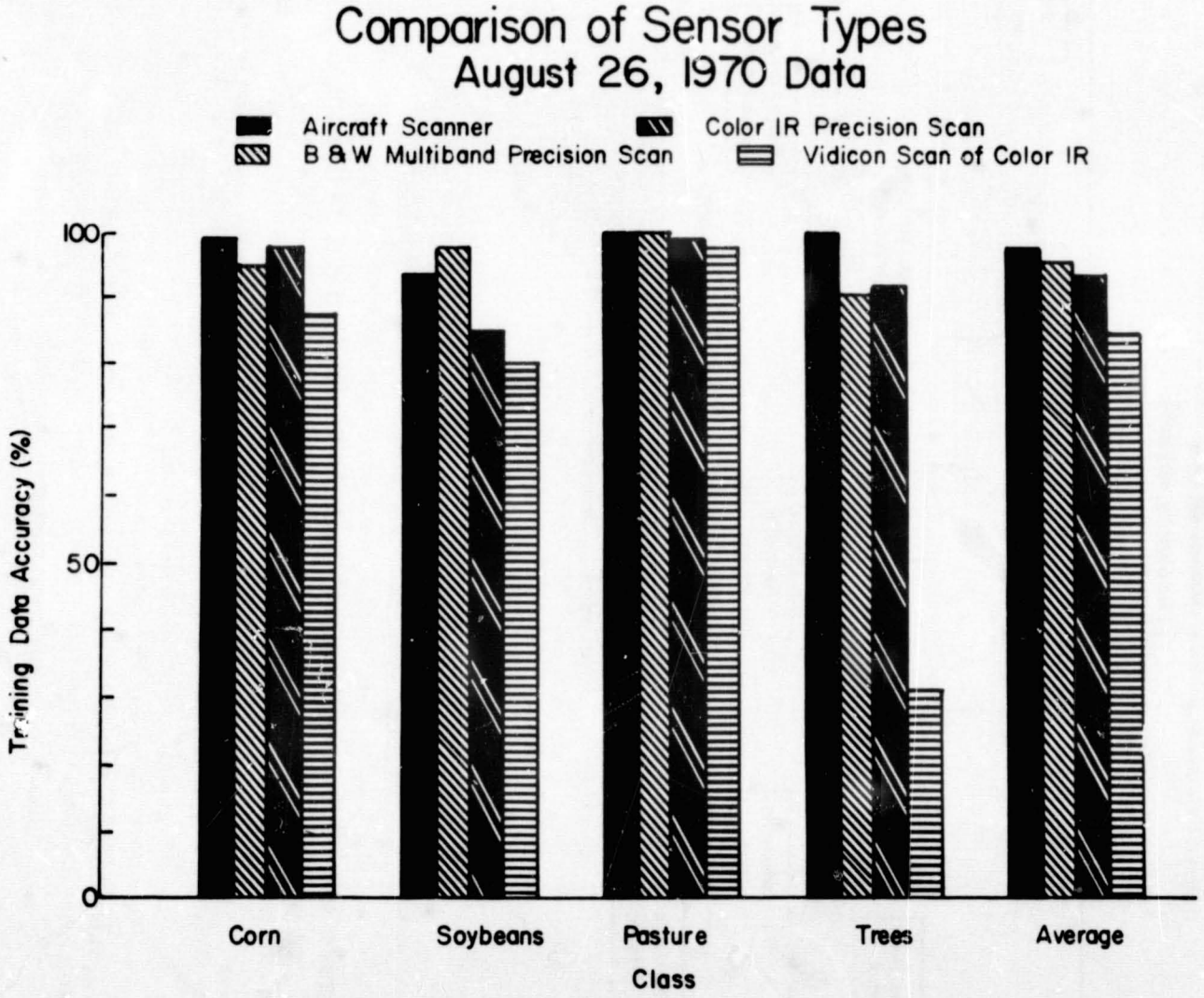

Figure 1.- Results of comparative classifications of multispectral data from four sensor types.

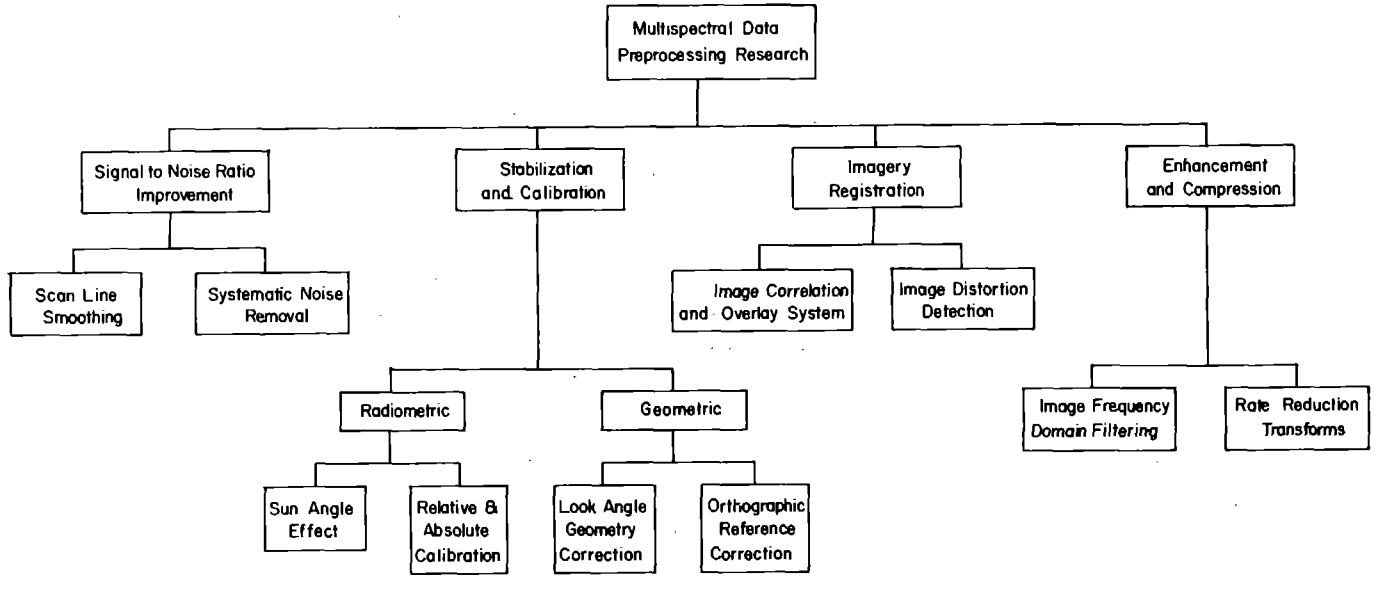

Figure 2.- Organization of multispectral data preprocessing studies being pursued at LARS/Purdue at this time.

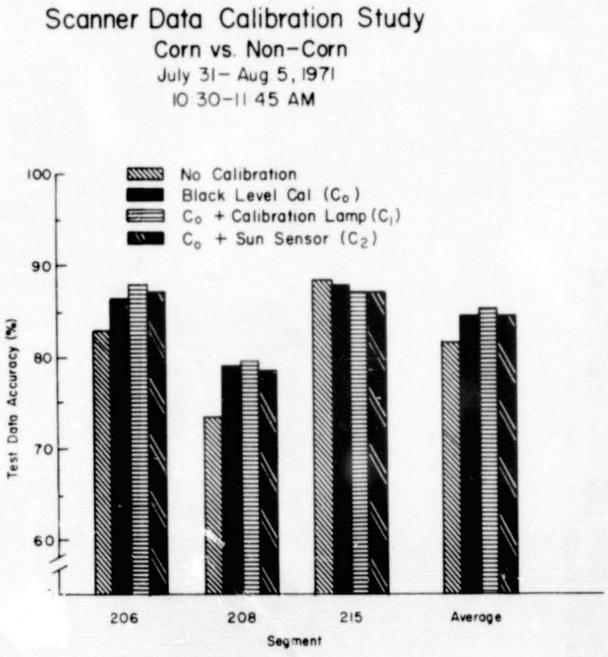

Figure 3.- Results of classifications from three different flightlines comparing four different calibration procedures.

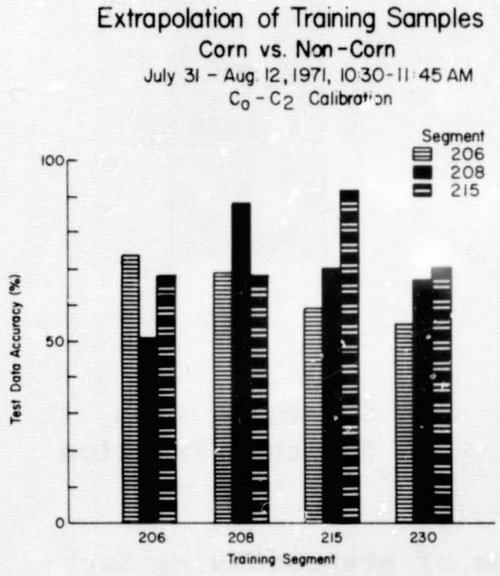

Figure 4.- Results of a test of extrapolating training data from one flightline to another. Segment 206 is more than 200 miles from segment 230, however, several factors, in addition to distance, are significant in this test.

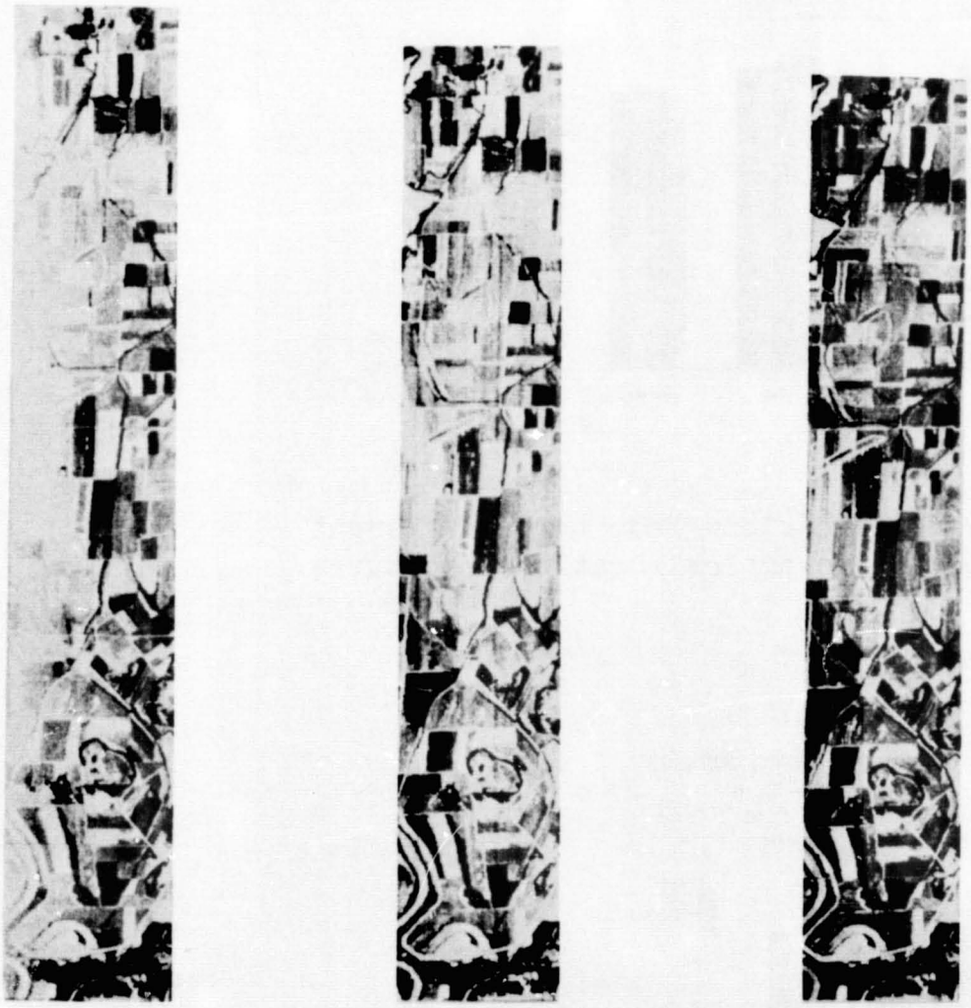

Uncorrected | Corrected | Corrected with Smoothed Function

Figure 5. An illustration of the use of preprocessing techniques to improve the appearance of imagery affected by variation in reflectance due to view angle and sun angle relationships (channel 6, segment 221, mission 42M, July 27, 1971.

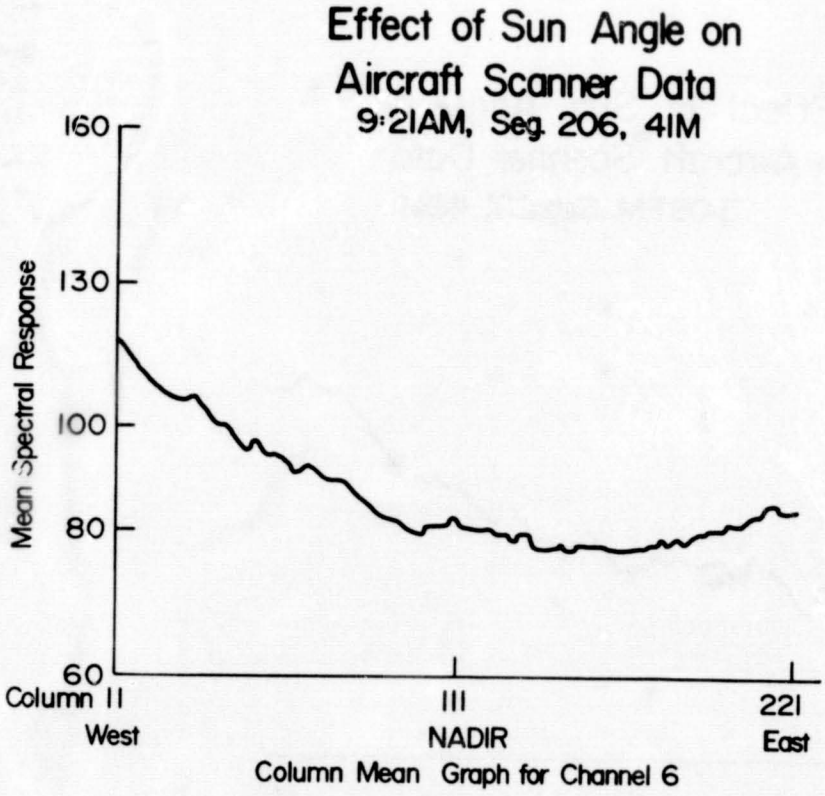

Figure 6.- A graph showing the mean spectral response as a function of view angle for data collected with an early morning sun angle. In this case, sufficient data has been used to nearly average out effects due to individual surface cover materials leaving only the sun angle effect.

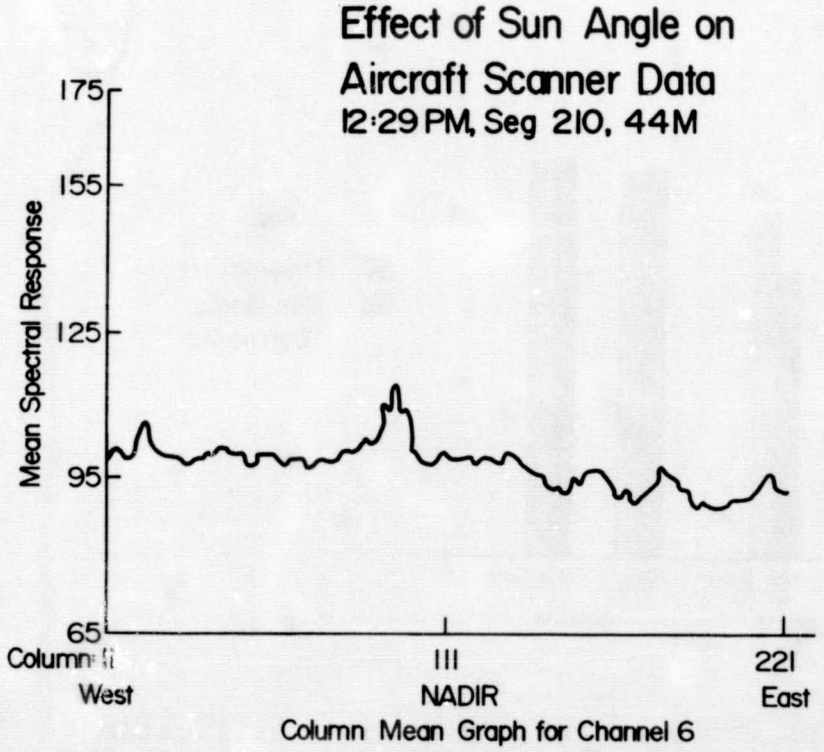

Figure 7.- A graph similar to Figure 6, but for data gathered with a nearly local noon sun angle.

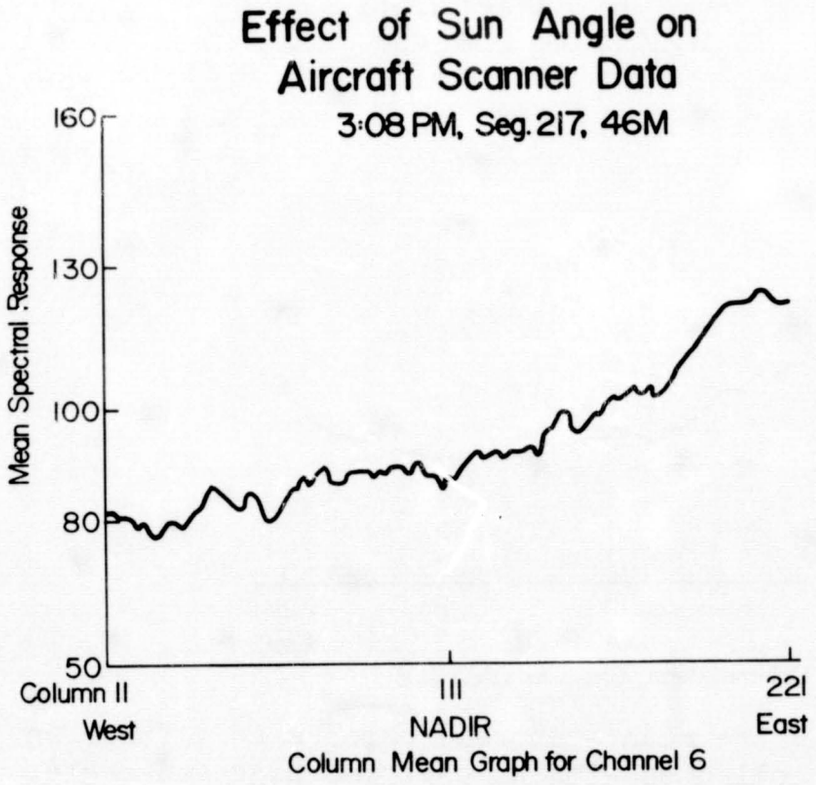

Figure 8.- A graph similar to Figure 6, but for data gathered with a late afternoon sun angle.

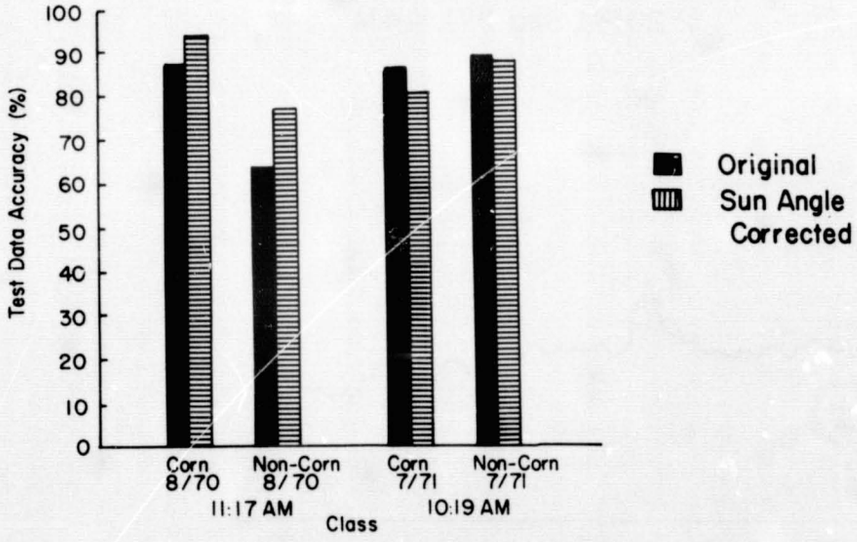

Figure 9.- Results of two corn vs. non-corn classifications carried out on the original data and the sun angle correction procedure used in Figure 5. Though the imagery appearance is obviously improved, the results from the quantitative classification comparison are mixed.

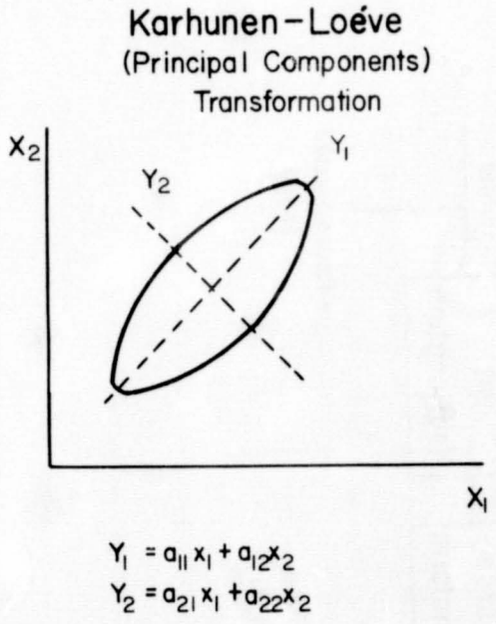

Figure 10.- A sketch of hypothetical bivariant multispectral data illustrating the result of a principal component transformation. X_1 and X_2 were the original coordinate axes; Y_1 and Y_2 are the new ones. The necessary equations are at the bottom.

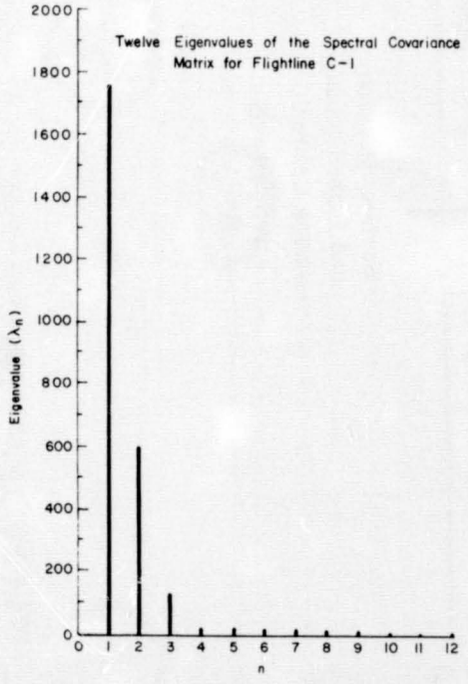

Figure 11.- The eigenvalues of an actual 12-band multispectral data set. An eigenvalue in this case is an indicator of the relative range of the data after principal components transformation. Even though there were 12 bands before transformation, only three appear to have significant range after.

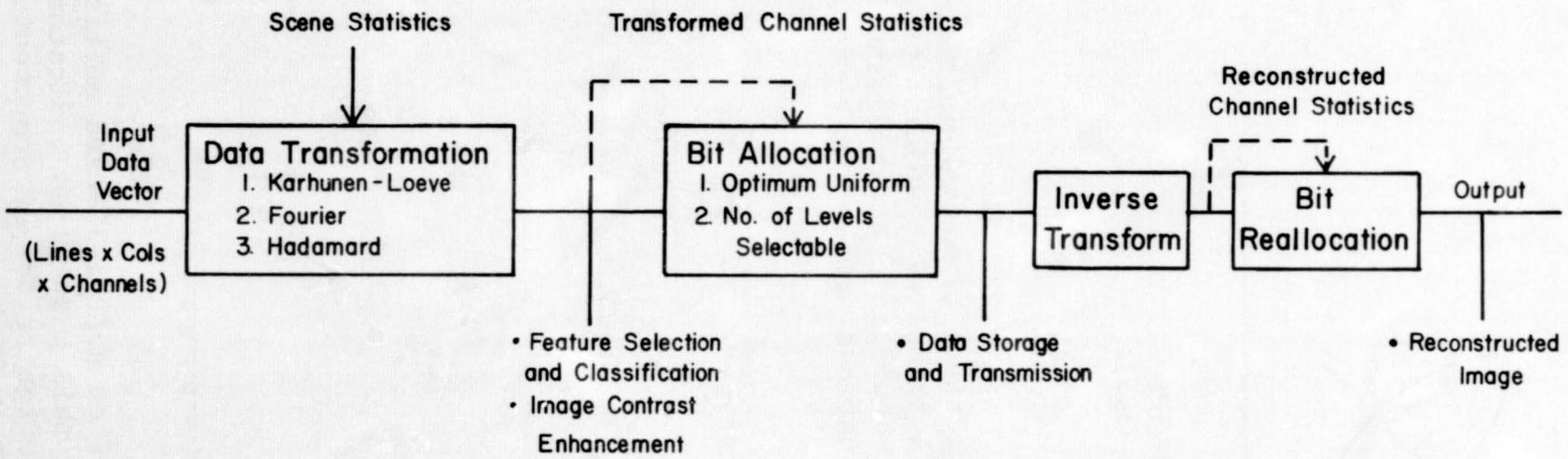

Figure 12.- Organization of a system used to test data compression transforms. Fourier and Hadamard transforms have been implemented in addition to the Karhunen-Loeve.

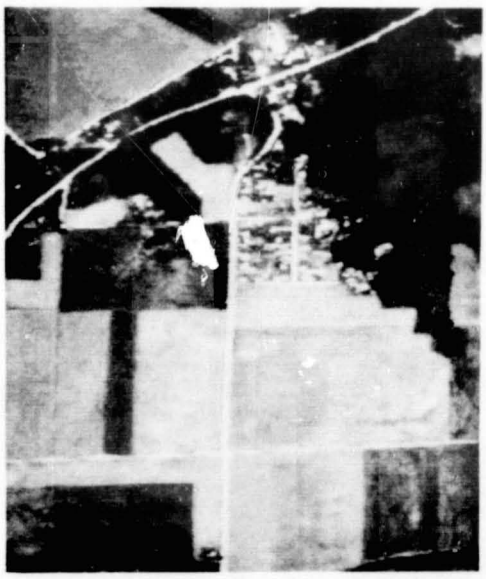

First Component

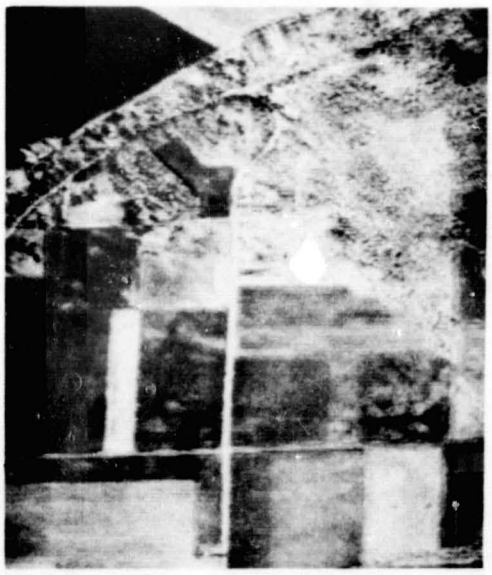

Second Component

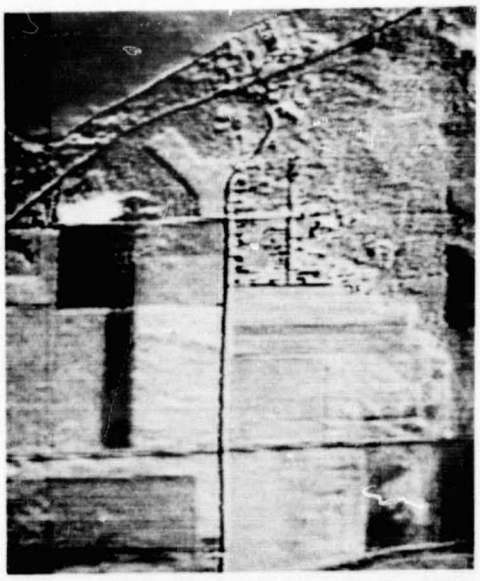

Third Component

Twelfth Component

Figure 13. Images generated after the data has first undergone principal components transform. The first two have higher contrasts than any of the original 12 spectral bands.

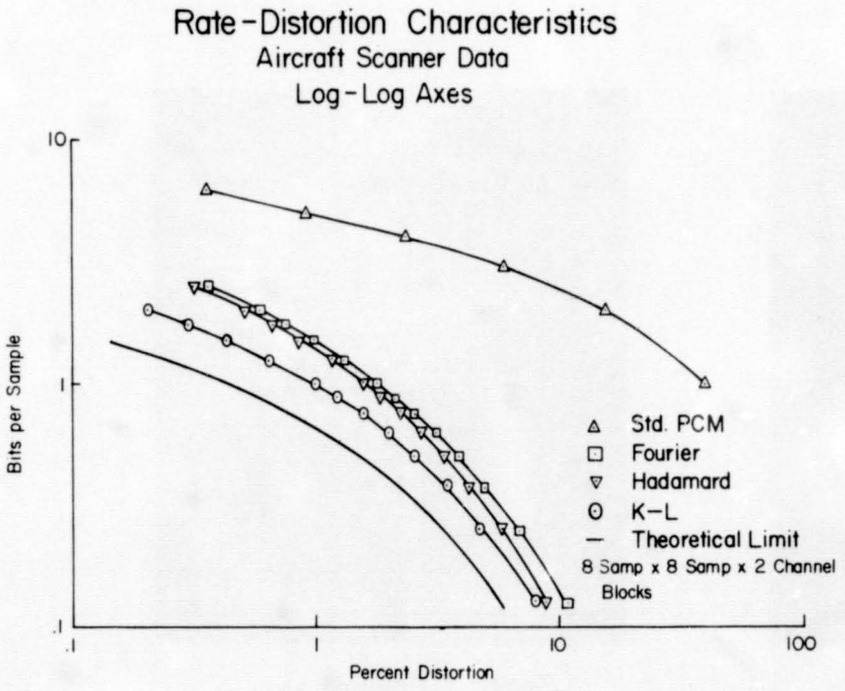

Figure 14.- Comparative rate distortion characteristics for the three transformations tested. Distortion is measured as the mean square difference between the original image and the compressed and reconstructed version.

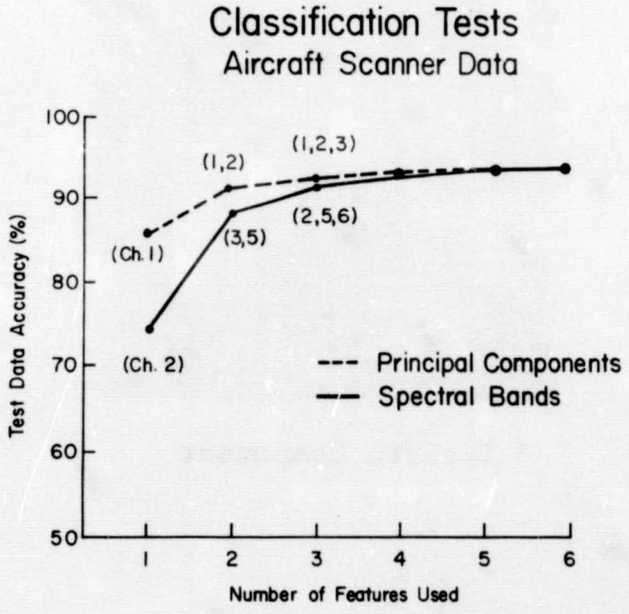

Figure 15.- Comparative results between classifications using original data and identical ones using principal components data. The best subsets of spectral bands were selected using a divergence processor.

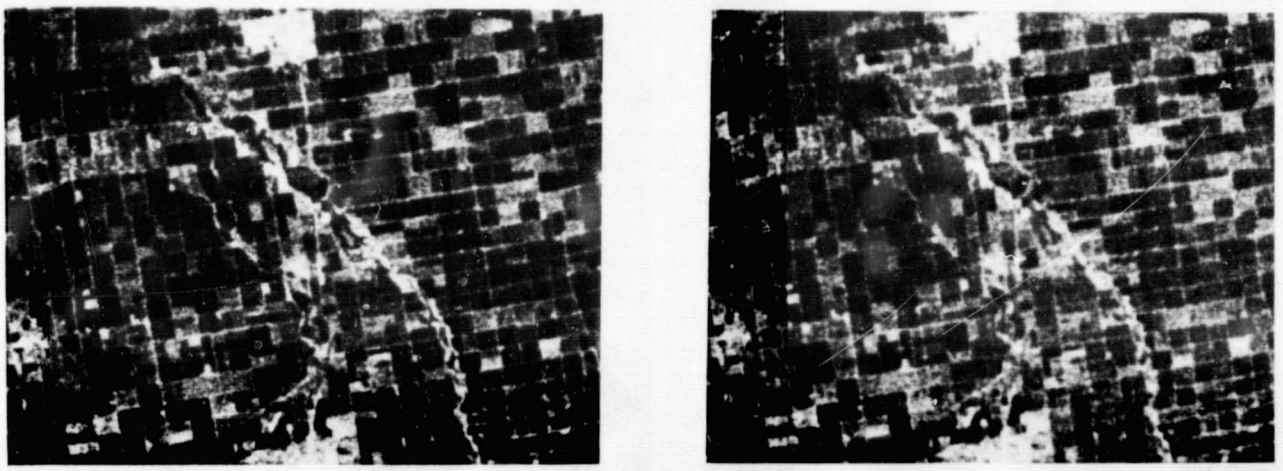

Original

8 X Compression

Figure 16. The results of data compression on image quality. A compression factor of 8 to 1 was used (Apollo 9 Frame No. 3698A).

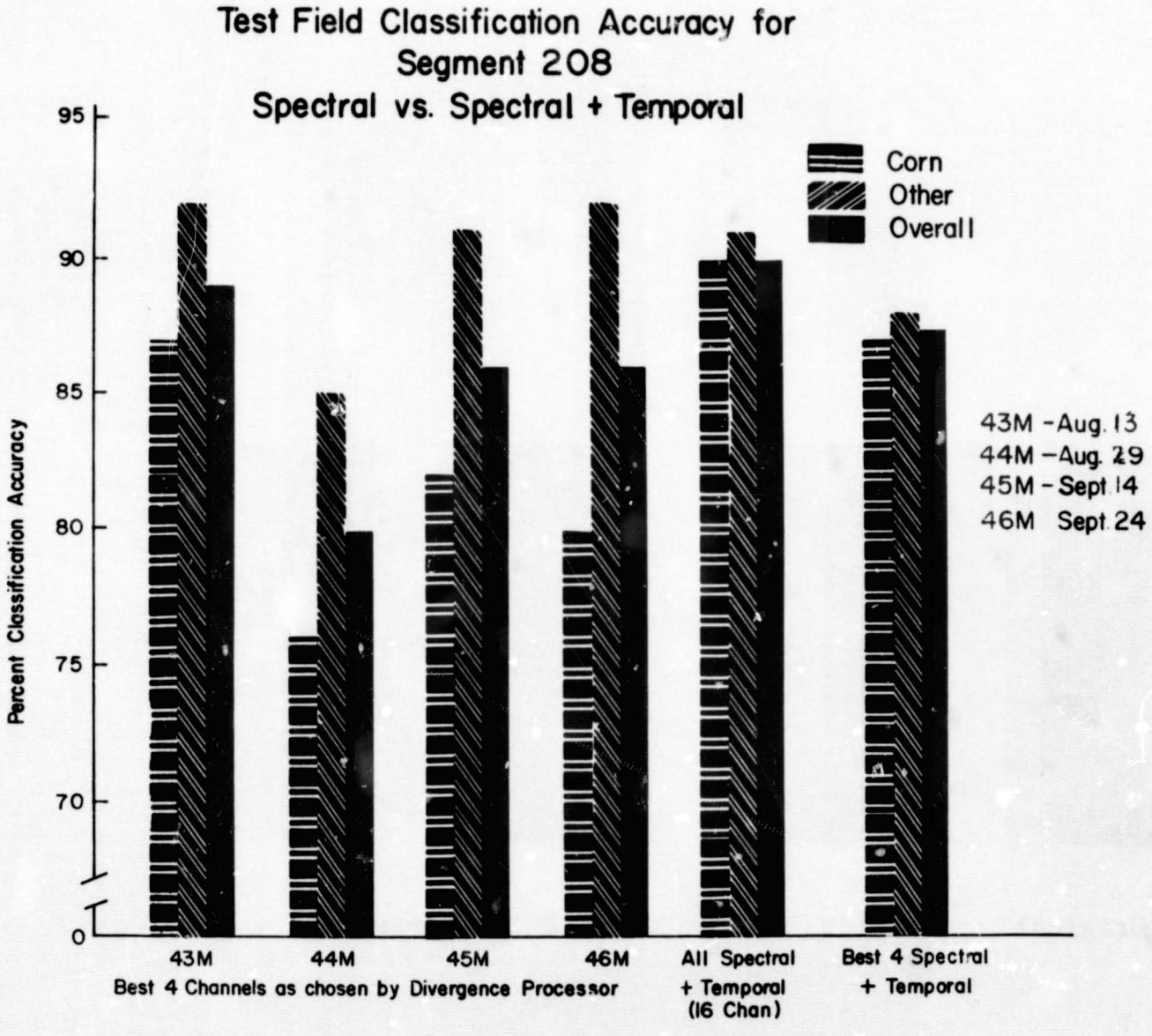

Figure 17.- A group of classification results illustrating the relative value of temporal information. The numbers 43M-46M are mission numbers flown on the dates shown.

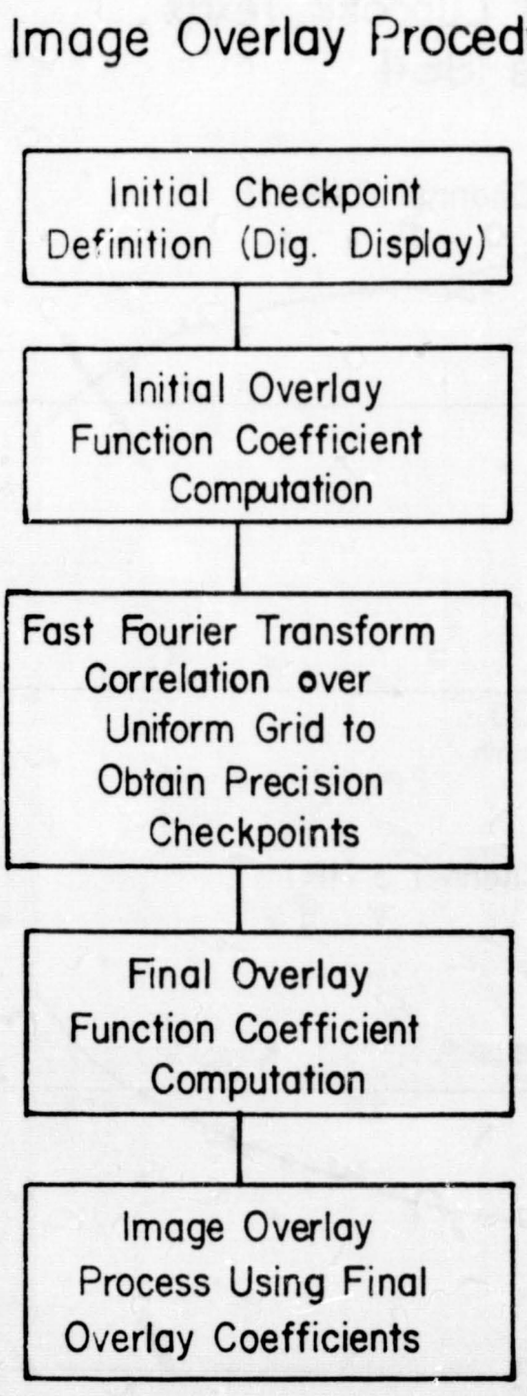

Figure 18.- The steps used in the current image overlay system.

Apollo 9 Digitized Image Correlation

Frame 3808 Lubbock, Texas
Line 1864

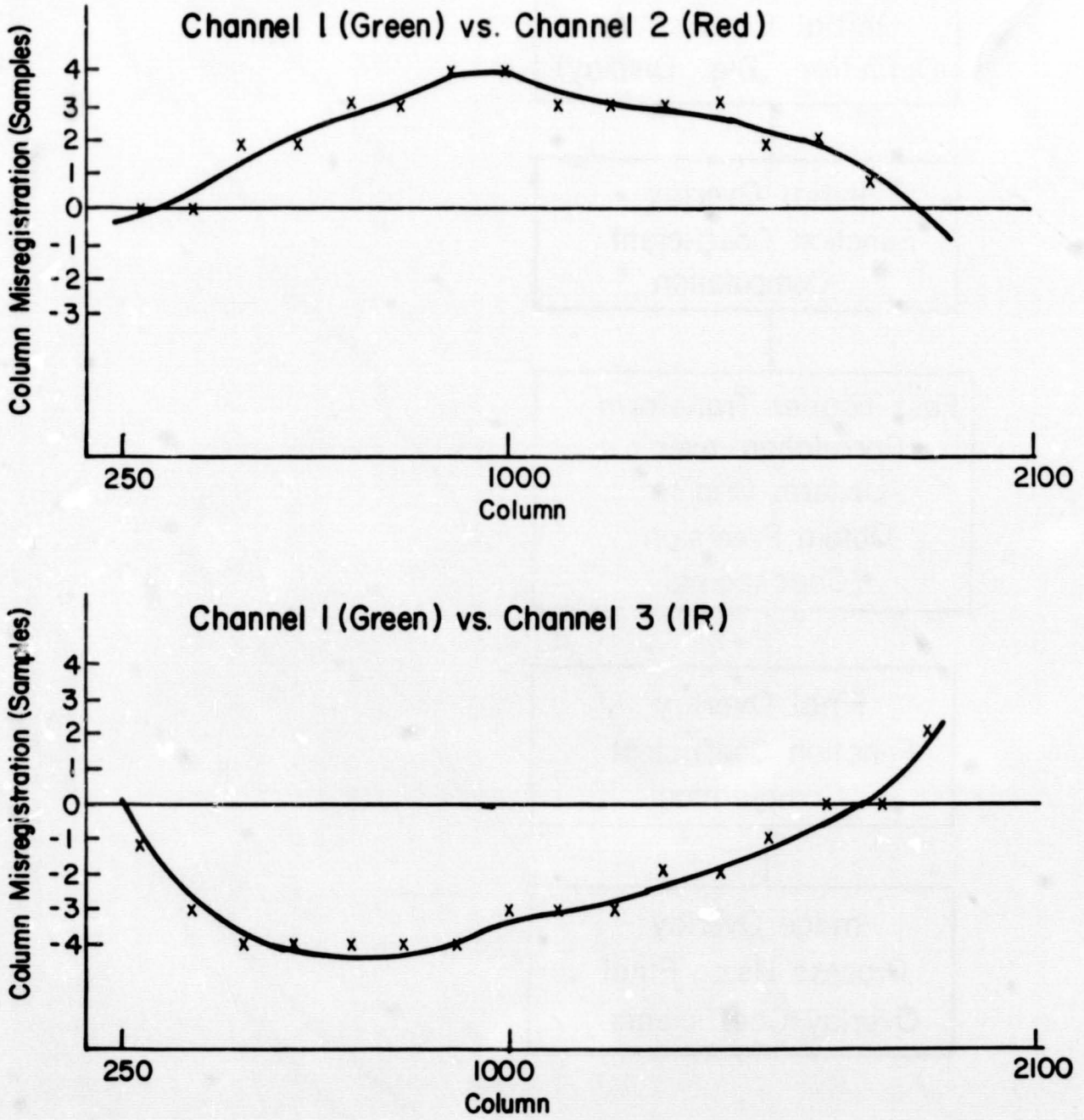

Figure 19.- Curves obtained with the image overlay system. They show that even when the particular frames were properly aligned at the left and right edges, they were as much as four samples (out of 2100) out of alignment in the middle. Thus, before overlaying a translation of the center portion of one image with respect to the other must be carried out in each case.

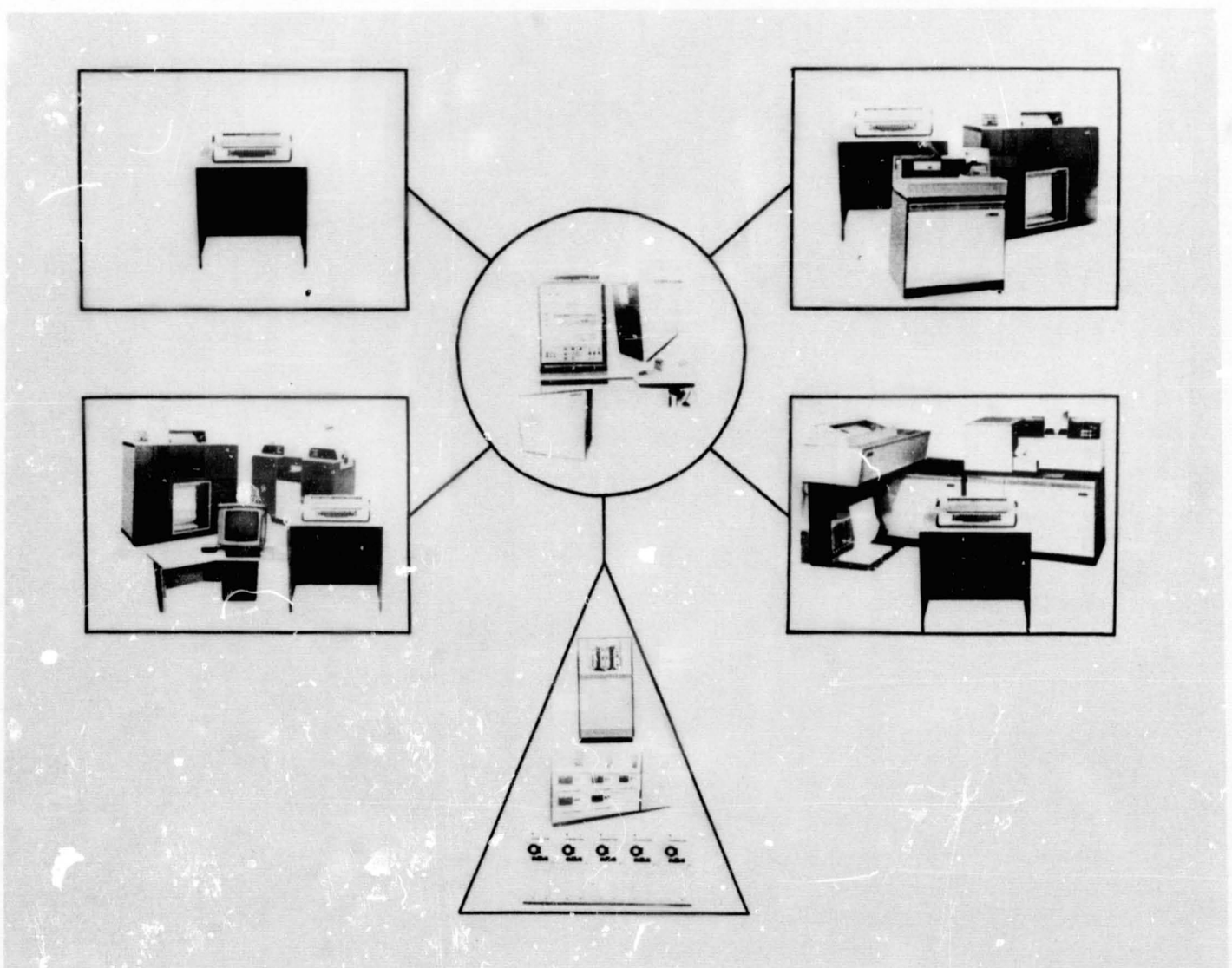

Figure 20.- The layout of equipment for the Multiterminal Processing System Experiment. The experiment will test the feasibility of centralizing the data bank and computational facility while proving input-output and control of that computational facility at multiple remote locations.